KCND3 potassium channel gene variant confers susceptibility to electrocardiographic early repolarization pattern

Alexander Teumer[1,2*], Teresa Trenkwalder[3*], Thorsten Kessler[3], Yalda Jamshidi[4], Marten E. van den Berg[5], Bernhard Kaess[6], Christopher P. Nelson[7,8], Rachel Bastiaenen[9], Marzia De Bortoli[10], Alessandra Rossini[10], Isabel Deisenhofer[3], Klaus Stark[11], Solmaz Assa[12], Peter S. Braund[7,8], Claudia Cabrera[13,14,15], Anna F. Dominiczak[16], Martin Gögele[10], Leanne M. Hall[7,8], M. Arfan Ikram[5], Maryam Kavousi[5], Karl J. Lackner[17,18], Lifelines Cohort Study[19], Christian Müller[20], Thomas Münzel[18,21], Matthias Nauck[2,22], Sandosh Padmanabhan[16], Norbert Pfeiffer[23], Tim D. Spector[24], Andre G. Uitterlinden[5], Niek Verweij[12], Uwe Völker[2,25], Helen R. Warren[13,14], Mobeen Zafar[12], Stephan B. Felix[2,26], Jan A. Kors[27], Harold Snieder[28], Patricia B. Munroe[13,14], Cristian Pattaro[10], Christian Fuchsberger[10], Georg Schmidt[29,30], Ilja M. Nolte[28], Heribert Schunkert[3,30], Peter Pramstaller[10], Philipp S. Wild[31], Pim van der Harst[12], Bruno H. Stricker[5], Renate B. Schnabel[20], Nilesh J. Samani[7,8], Christian Hengstenberg[32], Marcus Dörr[2,26], Elijah R. Behr[33], Wibke Reinhard[3]

1 Institute for Community Medicine, University Medicine Greifswald, Germany
2 DZHK (German Center for Cardiovascular Research), partner site Greifswald, Greifswald, Germany
3 Klinik für Herz- und Kreislauferkrankungen, Deutsches Herzzentrum München, School of Medicine, Technical University of Munich, Munich, Germany
4 Genetics Research Centre, Institute of Molecular and Clinical Sciences, St George's University of London, United Kingdom
5 Department of Epidemiology, Erasmus MC - University Medical Center Rotterdam, The Netherlands
6 Medizinische Klinik I, St. Josefs-Hospital, Wiesbaden, Germany
7 Department of Cardiovascular Sciences, Cardiovascular Research Centre, Leicester, Leicester, United Kingdom
8 NIHR Leicester Biomedical Research Centre University of Leicester, Leicester, United Kingdom
9 Cardiology Clinial Academic Group, Institute of Molecular and Clinical Sciences, St George's, University of London, United Kingdom
10 Institute for Biomedicine, Eurac Research, affiliated with the University of Lübeck, Bolzano, Italy
11 Department of Genetic Epidemiology, University Regensburg, Germany
12 Department of Cardiology, University of Groningen, University Medical Center Groningen, The Netherlands
13 Clinical Pharmacology, William Harvey Research Institute, Barts and The London, Queen Mary University of London, London, UK
14 NIHR Barts Cardiovascular Biomedical Research Centre, Barts and The London School of Medicine and Dentistry, Queen Mary University of London, London, UK
15 Centre for Translational Bioinformatics, William Harvey Research Institute, Barts and the London School of Medicine and Dentistry, Charterhouse Square, London, UK
16 Institute of Cardiovascular and Medical Sciences, College of Medical, Veterinary and Life Sciences, University of Glasgow, Glasgow, Scotland, UK
17 Institute of Clinical Chemistry and Laboratory Medicine, University Medical Center of the Johannes Gutenberg-University Mainz, Mainz, Germany
18 German Center for Cardiovascular Research (DZHK), partner site RhineMain, Mainz, Germany
19 The list of the Lifelines Cohort Study group authors is provided in the study acknowledgments
20 Department of General and Interventional Cardiology, University Heart Center Hamburg-Eppendorf, Germany, DZHK (German Center for Cardiovascular Research), partner site Hamburg/Kiel/Lübeck, Germany
21 Center for Cardiology - Cardiology I, University Medical Center of the Johannes Gutenberg-University Mainz, Mainz, Germany
22 Institute of Clinical Chemistry and Laboratory Medicine, University Medicine Greifswald, Greifswald, Germany
23 Department of Ophthalmology, University Medical Center of the Johannes Gutenberg-University Mainz, Mainz, Germany
24 Department of Twin Research and Genetic Epidemiology, King’s College London, London, UK
25 Interfaculty Institute for Genetics and Functional Genomics, University Medicine Greifswald, Greifswald, Germany
26 Department of Internal Medicine B, University Medicine Greifswald, Greifswald, Germany
27 Department of Medical Informatics, Erasmus MC - University Medical Center Rotterdam, The Netherlands

28 Department of Epidemiology, University of Groningen, University Medical Center Groningen, Groningen, The Netherlands
29 Innere Medizin I, Klinikum rechts der Isar, Technical University Munich, Munich, Germany
30 Deutsches Zentrum für Herz- und Kreislauf-Forschung (DZHK) e.V. (German Center for Cardiovascular Research), Partner Site Munich Heart Alliance, Munich, Germany
31 Preventive Cardiology and Preventive Medicine, Center for Cardiology, University Medical Center of the Johannes Gutenberg-University Mainz, Mainz, Germany; Center for Thrombosis and Hemostasis, University Medical Center of the Johannes Gutenberg-University Mainz, Mainz, Germany; DZHK (German Center for Cardiovascular Research), partner site Rhine-Main, Mainz, Germany
32 Division of Cardiology, Department of Internal Medicine II, Medical University of Vienna, Vienna, Austria
33 Cardiology Clinical Academic Group, Institute of Molecular and Clinical Sciences, St George's, University of London, United Kingdom AND St George's University Hospitals NHS Foundation Trust, London, United Kingdom

* These authors contributed equally to this work.

Corresponding Author:
PD Dr. med. Wibke Reinhard
Klinik für Herz- und Kreislauferkrankungen
Deutsches Herzzentrum München, Technische Universität München
Lazarettstrasse 36
80636 München
Germany
tel: +49 89 1218 4025
email: w.hengstenberg@dhm.mhn.de

Abstract

Background. The presence of an early repolarization pattern (ERP) on the surface electrocardiogram (ECG) is associated with risk of ventricular fibrillation and sudden cardiac death. Family studies have shown that ERP is a highly heritable trait but molecular genetic determinants are unknown.

Methods. To identify genetic susceptibility loci for ERP, we performed a GWAS and meta-analysis in 2,181 cases and 23,641 controls of European ancestry.

Results. We identified a genome-wide significant (p<5E-8) locus in the *KCND3* (potassium voltage gated channel subfamily D member 3) gene that was successfully replicated in additional 1,124 cases and 12,510 controls. A subsequent joint meta-analysis of the discovery and replication cohorts identified rs1545300 as the lead SNP at the *KCND3* locus (OR 0.82 per minor T allele, p=7.7E-12), but did not reveal additional loci. Co-localization analyses indicate causal effects of *KCND3* gene expression levels on ERP in both cardiac left ventricle and tibial artery.

Conclusions. In this study we identified for the first time a genome-wide significant association of a genetic variant with ERP. Our findings of a locus in the *KCND3* gene not only provide insights into the genetic determinants but also into the pathophysiological mechanism of ERP, discovering a promising candidate for functional studies.

Funding. For detailed information per study, see Acknowledgments.

Introduction

The early repolarization pattern (ERP) is a common ECG finding characterized by an elevation at the QRS-ST junction (J-point) of at least 0.1 mV in two adjacent ECG leads. The prevalence of ERP in the general population ranges from 2 to 13% being more common in young athletic men(1–5). The classical notion of ERP being a benign ECG phenotype was challenged in 2008 by the landmark study of Haissaguerre and colleagues showing an association of ERP with increased risk of ventricular fibrillation and sudden cardiac death(6): the Early Repolarization Syndrome (ERS)(7). Since then several studies demonstrated an elevated risk of cardiovascular and all-cause mortality in individuals with ERP underscoring its arrhythmogenic potential(2, 8, 9). Although the mechanistic basis for malignant arrhythmias in ERS is unclear, it has been suggested that they occur as a result of an augmented transmural electrical dispersion of repolarization(10). Ex vivo studies point towards a central role of the cardiac transient outward potassium current (I_{to}) in the development of both, ERP and ERS(11). Furthermore, candidate genetic association studies have highlighted a role for several genes encoding cardiac ion channels in the development of ERP and ERS(12–15). These genes include gain-of-function variants in I_K-ATP channels (*KCNJ8*, *ABCC9*) and loss-of-function variants in cardiac L-type calcium channels (*CACNA1C*, *CACNB2b*, *CACNA2D1*) and sodium channels (*SCN5A*, *SCN10A*)(16). Interestingly, co-existence of two genetic variants in different ion channel genes with opposing effects can be observed leading to phenotypic incomplete penetrance of ERP(15). However, data from functional studies confirming causality are scarce(17).

Studies among relatives of sudden arrhythmic death syndrome show that ERP is more prevalent in the relatives than in controls indicating that ERP is an important potentially inheritable pro-arrhythmic trait(18, 19). Moreover, in family studies the heritability estimate for the presence of ERP was h^2=0.49 (20). However, estimates for common SNP heritability from unrelated individuals are lower(21). This may explain why the only GWAS on ERP to date failed to identify genetic variants reaching genome-wide significance(22), and indicates the need for larger GWAS with more power.

In order to identify genetic variations that convey susceptibility to ERP we performed a GWAS and meta-analysis in European ancestry individuals, comprising 2,181 ERP cases and 23,641 controls from eight cohorts that formed the discovery stage. The findings were taken forward to a replication stage in 1,124 cases and 12,510 controls from four additional cohorts. To maximize statistical power

for locus discovery, we subsequently performed a combined discovery and replication cohort GWAS meta-analysis of 3,305 ERP cases and 36,151 controls.

Results

Clinical characteristics of the study cohorts are depicted in **Table 1**. The proportion of ERP based on the definition by Haisaguerre and Macfarlane(6, 23) ranged from 6% to 14% which is in line with previously reported prevalence in the general population(2–4).

Novel variants associated with ERP

In the first stage, we performed a GWAS meta-analysis in up to 2,181 cases and 23,641 controls from eight discovery cohorts. In total, 6,976,246 SNPs passed quality control (see Methods). We identified 19 variants spanning 49 kb in *KCND3* (Potassium Voltage-Gated Channel Subfamily D Member 3) as well as rs139772527 (effect allele frequency [EAF] 1.4%, OR=2.57, p=2.0E-8) near *HBZ* (Hemoglobin Subunit Zeta) to be genome-wide significantly associated (p<5E-8) with ERP. The SNP with the lowest p-value in the region (the lead SNP) at *KCND3* was the intronic rs12090194 (EAF 32.5%, OR=0.80, p=4.6E-10), and was replicated in an independent sample of 1,124 cases and 12,510 controls from four additional cohorts ($p_{replication}$=2.5E-3, $p_{combined}$=9.3E-12, **Table 2**). The SNP rs139772527 near *HBZ* did not fulfil the criteria for replication ($p_{replication}$=0.28, $p_{combined}$=1.4E-6, **Table 2**) as described in the Methods. The subsequent combined meta-analysis of all 12 cohorts including up to 39,456 individuals revealed only the locus at *KCND3* to be genome-wide significantly associated with ERP (**Supplementary Figure 1**). The lead SNP of the combined GWAS meta-analysis was rs1545300 (EAF 31.9%, OR=0.82, p=7.7E-12), followed by the discovery stage lead SNP rs12090194 being in strong linkage disequilibrium with rs1545300 (r^2=0.96, D'=1) (**Figure 1**). Both SNPs were imputed at very high confidence (imputation quality score >0.97) in all cohorts. The quantile-quantile plots did not show any inflation (individual study λ_{GC} between 0.81 and 1.03, median: 0.91), and overall meta-analysis λ_{GC}=1.02 (linkage disequilibrium [LD] score regression intercept: 1.01, see Methods) (**Supplementary Figure 2**). The result of the combined GWAS meta-analysis was used for the subsequent analyses. Summary statistics based conditional analysis to select independent hits did not reveal any secondary signals. The association results for each stage of the lead SNPs with p<1E-6 in the discovery meta-analysis are provided in **Supplementary Table 1**.

Statistical finemapping of the associated locus

All significantly associated SNPs of the combined GWAS meta-analysis were located within *KCND3*, the potassium voltage-gated channel subfamily D member 3 gene, and were intronic (**Table 3, Figure 2**). We used these results to assess whether a single SNP or set of variants drive the association signal in *KCND3* (credible set). The 99% credible set was computed based on Approximate Bayes Factors for each SNP, resulting for each in a set of SNPs that with 99% posterior probability contained the variant(s) driving the association signal. For the associated locus at *KCND3* the credible set spanned 49 kb, and contained 19 variants. The two lead SNPs rs1545300 and rs12090194 had a posterior probability of 21% and 19%, respectively, whereas the former candidate SNP rs17029069(22) had a posterior probability of 2% (**Supplementary Table 2**).

To test whether the association in *KCND3* might be driven by heart rate or RR interval, we performed a sensitivity analysis in the 1,253 ERP cases and 11,463 controls of the Lifelines cohort adjusting the genetic association of rs1545300 additionally for these two traits in separate models. The effect estimates were virtually unchanged (OR=0.78) with p=1.2E-7 for both adjustments. In addition, we assessed whether the association of rs1545300 might be related to a specific ERP subtype i.e. ST segment or ERP localization. In all subtype-stratified analyses the 95% confidence intervals of the effect sizes overlapped with the overall results not pointing to a subtype driven signal (**Supplementary Table 3**).

Expression quantitative trait locus (eQTL) and co-localization

We searched the Genotype-Tissue Expression (GTEx) project database(24) to look for tissue-specific eQTLs including all genes in vicinity of ±1Mb of the lead SNP rs1545300 and found an association with *KCND3* expression levels in tibial artery (p=3.0E-6, n=388). Two additional eQTL associations of rs1545300 at FDR<0.2 across the 48 tissues tested were found with *KCND3* (ENSG00000171385.5) in the left ventricle (p=2.9E-4, n=272) of the human heart, and with *CEPT1* (ENSG00000134255.9) in the minor salivary gland (p=3.4E-4, n=85) (**Supplementary Table 4**).

Subsequent co-localization analyses of rs1545300 in these three tissues revealed also a significant correlation of gene expression pattern with ERP ($p_{SMR} \leq 0.01$) (**Figure 3**, **Supplementary Table 5**), where for the left ventricle the correlation seems to be attributable to the same underlying causative variant ($p_{HEIDI} \geq 0.05$), and for tibial artery the test was close to nominal significance ($p_{HEIDI}=0.05$). However, the significant $p_{HEIDI}=1.7E-3$ of *CEPT1* in the minor salivary gland points rather towards a pleiotropic effect of rs1545300 than to a causal effect of gene expression on ERP in this tissue. For all

three tissues, an increased gene expression level was associated with a higher risk of ERP (**Supplementary Table 5**).

Pleiotropic effects of the lead SNPs

To assess pleiotropic effects of the *KCND3* lead SNP rs1545300 or its proxies (r^2>0.8), we looked for genome-wide significant associations in the NHGRI-EBI Catalog of published genome-wide association studies(25) (accessed: 07/30/2019). Pleiotropic associations were found for P-wave terminal force (rs12090194 and rs4839185)(26) and for reduced risk of atrial fibrillation per minor allele (rs1545300 and rs1443926)(27, 28). All these SNPs were in strong linkage disequilibrium (r^2>0.97) with the lead SNP. In addition, variants in low to moderate LD with rs1545300 were associated with P-wave duration (rs2798334, r^2=0.26)(29) and ST-T-wave amplitudes (rs12145374, r^2=0.60)(30). A phenome-wide lookup of rs1545300 in the association results of 778 traits available via the Gene ATLAS web portal (31) using 452,264 individuals of the UK Biobank cohort revealed an association of the ERP risk reducing minor T allele with reduced risk of heart arrhythmia (estimated OR=0.92, p=3.6E-6). Of note, no other of the assessed traits reached significance after Bonferroni correction (p<0.05/778=6.4E-5).

Discussion

In this GWAS meta-analysis comprising 3,305 cases and 36,151 controls including independent replication samples, we describe an association of ERP with a locus on chromosome 1 in the *KCND3* gene. This is the first study identifying a robust genome-wide significant association between genetic variants and ERP. Our findings provide a candidate gene for further functional studies examining the pathophysiological mechanism of ERP and potentially ERS. The *KCND3* gene encodes the main pore-forming alpha subunit of the voltage-gated rapidly inactivating A-type potassium channel. In the cardiac ventricle *KCND3* contributes to the fast cardiac transient outward potassium current (I_{to}), which plays a major role in the early repolarization phase 1 of the cardiac action potential (AP).

To date, two competing theories explain the presence of J waves and ERP: the repolarization and the depolarization theory, both involving the I_{to} channel. On the basis of animal models evidence for the former is more compelling. Thus, J waves result from a transmural voltage gradient created by a more prominent epicardial phase 1 AP notch relative to the endocardial AP notch(11, 32). The I_{to} current notably influences the degree of the transmural heterogeneity of the phase 1 AP notch and

consecutively the magnitude of the J wave(11, 32). Pharmacological inhibition of the I_{to} current with 4-aminopyridine results in a reduction of the J wave amplitude(11). The depolarization theory is based on clinical overlap of ERP with Brugada syndrome, which has led to the suggestion of Brugada syndrome being a right ventricular variant of the ERP(33). In theory, deviation from the sequential activation of cardiac currents I_{Na}, I_{to}, and I_{CaL} can lead to regional conduction slowing and appearance of inferior and/or lateral ERP(32, 34). In patients with ERS, distinct phenotypes of both delayed depolarization and early repolarization have been identified(35).

ERP is a highly heritable trait within families(3, 20), however limited heritability can be attributed to common SNPs in unrelated individuals(21). This might be a reason why the only GWAS to date which included 452 cases failed to replicate any genome-wide significant loci(22). In our study, which includes 3,334 cases, we discovered and replicated variants in the *KCND3* gene. Interestingly, one of these variants (rs17029069), which is in moderate LD (r^2=0.18, D'=-1) with our lead SNP rs1545300 (**Supplementary Figure 3**) was reported as a candidate in the earlier GWAS meta-analysis(22). However, this variant did not replicate in their study, which the authors attributed to limited power based on the small sample size and/or heterogeneous phenotyping. In our study, experienced cardiologists evaluated more than 39,000 ECGs with high reproducibility ensuring a very high phenotyping quality(21). The resulting homogenously assessed phenotype and the substantially increased number of cases are two aspects that elevated the statistical power of our GWAS meta-analysis. All detected variants cluster in intronic regions of the *KCND3* gene, without significant allelic heterogeneity. The annotation of the locus does not point to a direct pathogenic effect, i.e. a protein altering mutation, and also the statistical finemapping revealed no single SNP with a substantial posterior probability (e.g. >80%) of being causal. However, the latter approach has limitations of detecting rare causal variants due to imputation uncertainty and minimum minor allele frequency (MAF). Nevertheless, eQTL analysis suggested that the detected variants may affect gene expression of *KCND3*. Potential mechanisms include modification of gene expression via altered binding of transcription factors at *cis*-elements through enhancers or in DNaseI hypersensitivity regions (**Figure 2**). This is supported by the results of the test for co-localization showing an increase of ERP risk due to increased gene expression levels of *KCND3* in tissues of the human heart and tibial artery. Similar, pharmacological ex vivo data predict gain of function mutations in the I_{to} current to increase the overall transmural outward shift, leading to an increased epicardial AP notch and thereby inducing ERP in the

surface ECG(32). Additionally, in close proximity to the lead SNP rs1545300 a long non-coding RNA (lncRNA), KCND3 antisense RNA 1 (*KCND3-AS1*) is described. LncRNAs have been shown to physiologically influence gene regulation through various mechanism e.g. chromatin remodeling, control of transcription initiation and post-transcriptional processing(36, 37). On the other hand, dysregulation of lncRNA control circuits can potentially impact development of disease(38): a very prominent example in cardiovascular diseases is the lncRNA *ANRIL*, which is a key effector of *9p21* in atherosclerotic risk and cardiovascular events(38–40).

Given the high prevalence of ERP in the general population and a high MAF of the identified genetic variants in our study the key question remains why only a very small subset of individuals develops severe ventricular arrhythmias and ERS. The fine interplay of a genetic predisposition and specific precipitating conditions might lead to an electrically vulnerable cardiac state. Insights into the potential origin of ventricular arrhythmias in ERS come from animal models and highlight the role of different ion channels including I_{to}(10). A pharmacological model of ERS in canine wedges from the inferior and lateral ventricular wall showed marked regional dispersion of repolarization (loss of phase 2 AP dome and AP shortening in some epicardial regions but not others). Presence of transmural repolarization heterogeneity allowed local re-excitation in form of closely coupled extrasystolic activity (phase 2 re-entry). The combination of an arrhythmogenic substrate, represented by regional electrical instability, and triggering premature ventricular beats resulted in ventricular fibrillation(10). Human data in ERS patients suggest that in a subgroup, the ERP is due to a pure repolarization phenotype and arrhythmia(35) is triggered by Purkinje fiber ectopic beats.

Genetic variants in various ion channel genes have been associated with ERS(16) including the *KCNJ8* and *ABCC9* genes encoding the Kir6.1 and ATP-sensing subunits of the K_{ATP} channel(6, 12, 41, 42). The commonly implicated variant KCNJ8-p.S422L has a population frequency not consistent with ERS, and is predicted to be benign by multiple in silico algorithms according to the ClinVar database(43). A recent study by Chauveau *et al.* has, however, identified a de novo duplication of the *KCND3* gene in a patient who survived sudden cardiac death and in his 2-year-old daughter(13). Both exhibited marked ERP in the inferolateral leads that was augmented by bradycardia and pauses in heart rhythm, in keeping with a repolarization mechanism underlying the ERS phenotype. Studies have suggested that the inferior region of the left ventricle has a higher density of *KCND3* expression and higher intrinsic levels of I_{to}(10). This may explain the higher vulnerability of this region for the

development of ERS in the setting of a genetically mediated gain-of-function in the I_{to} current. Moreover, observational studies also identified different ERP subtypes including the occurrence of ERP in the inferior region and a horizontal/descending ST segment morphology to be associated with a higher risk of sudden arrhythmic death and cardiovascular mortality(2, 44, 45). However, in a subgroup of our study the association signal of ERP risk and *KCND3* variation was not dominated by a specific ERP high-risk subtype. Of note the formation of subgroups led to reduction in sample size and thus statistical power.

Taken together, the rare occurrence of ERS may be explained by different conditions. On the one hand, an underlying monogenic mutation may be found in some cases. On the other, no single causal mutation can be identified in the majority of ERS cases rendering the influence of multiple genes and environmental factors more likely i.e. a 'multi-hit condition'. Similar to other polygenic diseases, the sum of multiple minor effects of several common genetic variations together with specific external triggers may affect the occurrence of ERS. There is indeed evidence to suggest that common variants in the *KCND3* locus increase arrhythmogenicity. A phenome-wide lookup of our common lead SNP in more than 450,000 individuals from the UK Biobank linked the minor T allele associated with reduced ERP to a reduced risk of heart arrhythmia(31). Furthermore, additional data show an association of the same common variant with reduced risk of atrial fibrillation(27, 28). A small effect of a common SNP at *KCND3* does not necessarily mean that the variant is benign; rather a single risk allele is associated with a small but effective change in the gene expression level. Thus, the overall effects of the *KCND3* gene expression levels on the phenotype may appear much stronger compared to the small effect of rs1545300. Based on our results, it could be hypothesized that variation in *KCND3* gene expression levels and subsequently its encoded protein may affect the risk of ERP and eventually ERS. The positive effect direction of the change in *KCND3* gene expression levels in heart tissue on the risk of ERP estimated via the SMR test (**Supplementary Table 5**) suggests an elevated risk with increasing abundance of the *KCND3* encoded protein. Functional validation is necessary to validate this hypothesis and analyses of the *KCND3* gene in individuals with ERS is warranted to confirm the role of *KCND3* variation in arrhythmogenesis.

Our study has some limitations, which need to be acknowledged. Presence of ERP in the ECG can be variable, as it has been described to be dependent on age, heart rate, vagal activity and medication, although our findings were valid after adjusting for some of these factors. Therefore, we cannot

exclude that we have missed some individuals with ERP. Second, the tissue-specific gene expression data used for the co-localization analysis is based on a limited sample size. A larger gene expression sample or functional studies are needed to validate the revealed effect of *KCND3* expression on the ERP. Also, we analyzed only common and low-frequency SNPs with a MAF >1% missing rare variants and variants not included in the imputation panel. Finally, long-term outcome data identifying those individuals with ERP who suffer from ERS are not available. Further GWAS in large international collaborative cohorts of ERS patients are therefore necessary to determine the genetic risk.

In conclusion, we show for the first time, a robust association of genetic variants with the ERP in a large GWAS of individuals of European ancestry. The locus in the *KCND3* ion channel gene is an intuitive candidate and supports the theory that at least a proportion of ERS is a pure channelopathy. Intensive future research will be needed to extend the discovery of ERP susceptibility loci to individuals of non-European ancestry, and to improve identification and risk stratification of the subset of individuals with the ERP who are at highest risk for potentially lethal ventricular arrhythmias.

Methods

Study cohorts and SNP genotyping

The discovery stage included 25,822 subjects (2,181 ERP cases) from eight independent cohorts with genetic and phenotypic data available for analyses: the British Genetics of Hypertension (BRIGHT) study, the Gutenberg Health Study (GHS1, GHS2), the Genetic Regulation of Arterial Pressure In humans in the Community (GRAPHIC) study, the Lifelines Cohort Study (Lifelines), the Study of Health in Pomerania (SHIP, SHIP-Trend), and TwinsUK. Additional 13,634 subjects (1,124 ERP cases) from four cohorts (Rotterdam Study I, II, III, and CHRIS) were used as independent replication: the Rotterdam Study (Rotterdam Study I, II, III), and the Cooperative Health Research In South Tyrol (CHRIS) study. The included subjects of all cohorts were of European ancestry, and all cohorts but BRIGHT (which sampled hypertensive cases) were population based (**Supplementary Table 6**). The determination of the discovery and replication cohorts was determined upfront based on the timeline of the availability of the genetic and ERP data.

Electrocardiogram analysis and ERP evaluation

12-lead ECGs of all 12 studies were obtained during a study visit in a supine position after approximately five minutes of rest and were analyzed manually by experienced and specifically trained

cardiologists for the presence of ERP. In detail, ECGs from TwinsUK and BRIGHT were evaluated in the UK (YJ, RB, ERB), ECGs from all other cohorts were evaluated in Germany (TT, BK, CH, WR). Paper-printed 12-lead ECGs were independently read by two experienced clinicians who were blinded with respect to age and sex. There was very high level of agreement between each pair of interpreters (95-98%)(20, 21). Cases of ambiguous or unequal phenotype were jointly reassessed by two readers, and a consensus decision was achieved. To determine interobserver variability between UK and German teams, a subset of ECGs was analyzed by both teams yielding a concordance of 96%(20, 21).

The ERP phenotype was established according to the definition by Haissaguerre and Macfarlane(6, 23). ERP was defined as elevation of the J-point above the level of QRS onset of ≥0.1 mV in at least two corresponding leads. To avoid confusion or overlap with Brugada syndrome or arrhythmogenic right ventricular dysplasia, leads V1 to V3 were excluded from ERP scoring. In case of presence of ERP, region, either inferior (leads II, III, aVF), antero-lateral (leads I, aVL, V_4-V_6), or both, and the maximum amplitude of J-point elevation was documented. Further, the morphology of ERP was assessed as either notching, slurring or both as well as the ST segment according to Tikkanen and collegues(44) as either concave/rapidly ascending (>0.1 mV elevation 100 ms after J-point peak or persistently elevated ST segment >0.1 mV) or horizontal/descending (≤0.1 mV elevation within 100 ms after J-point peak)(23, 44). In case of a QRS duration of >120 ms or rhythm other than sinus rhythm (e.g. atrial fibrillation, pacemaker stimulation) ECGs were excluded from the analysis.

Statistics

Unless stated otherwise, the analyses were conducted and plotted using the R statistical software(46), a Z-test was applied, and all reported p-values are two-sided.

GWAS in individual studies

The GWAS in each study for both the discovery and replication stage was performed on autosomal imputed SNP genotypes using study-specific quality control protocols which are provided in detail in **Supplementary Table 6**. Association analyses were performed using logistic regression for ERP status as outcome and an additive genetic model on SNP dosages, thus taking genotype uncertainties of imputed SNPs into account. The analyses were adjusted for age, sex, and relevant study-specific covariates such as principal components for population stratification (**Supplementary Table 6**).

Meta-analysis of individual study GWAS results

The result files from individual studies GWAS underwent extensive quality control before meta-analysis using the gwasqc() function of the GWAtoolbox package v2.2.4(47). The quality control included file format checks as well as plausibility and distributions of association results including effect sizes, standard errors, allele frequencies and imputation quality of the SNPs.

The meta-analyses were conducted using a fixed-effect inverse variance weighting as implemented in Metal(48). Monomorphic SNPs, SNPs with implausible association results (i.e. p≤0, SE≤0, |log(OR)|≥1000), and SNPs with an imputation quality score ≤0.4 were excluded prior to the meta-analyses resulting in a median of 12,839,202 SNPs per cohort (IQR: 10,756,073-13,184,807). During the meta-analysis, the study-specific results were corrected by their specific λ_{GC} if >1. Results were checked for possible errors like use of incorrect association model by plotting the association p-values of the analyses against those from a z-score based meta-analysis for verifying overall concordance. SNPs that were present in <75% of the total sample size contributing to the respective meta-analysis or with a MAF ≤0.01 were excluded from subsequent analyses. Finally, data for up to 6,976,246 SNPs were available after the meta-analysis.

Quantile-quantile plots of the meta-analysis results are provided in **Supplementary Figure 2**. To assess whether there was an inflation of p-values in the meta-analysis results attributed to reasons other than polygenicity, we performed LD score regression(49). The LD score corrected λ_{GC} value of the discovery and replication combined meta-analysis was 1.01, supporting the absence of unaccounted population stratification. Genome-wide significance was defined as a p-value <5E-8, corresponding to a Bonferroni correction of one million independent tests(50). The I^2 statistic was used to evaluate between-study heterogeneity(51).

To evaluate the presence of allelic heterogeneity within each locus, the GCTA stepwise model selection procedure (cojo-slct algorithm) was used to identify independent variants employing a step-wise forward selection approach(52). We used the genotype information of 4,081 SHIP individuals for LD estimation, and set the significance threshold for independent SNPs to 5E-8.

All loci were named according to the nearest gene of the lead SNP. Genomic positions correspond to build 37 (GRCh37).

Replication analysis

To minimize the burden for multiple testing correction and thus maximizing the power for replication, the lead SNPs of genome-wide significant loci in the discovery stage were taken forward to the replication stage in independent samples (**Table 1**). SNPs were considered as replicated if the p-value

of a one-sided association test was <0.025 which corresponds to a Bonferroni correction for the two lead SNPs tested at 5% significance level.

Finally, the GWAS results from the discovery and replication studies were meta-analyzed to search for additional genome-wide significant loci by maximizing the statistical power for locus discovery.

Gene expression based analyses

The lead SNP rs1545300 of the *KCND3* locus of the combined discovery and replication GWAS meta-analysis was tested for *cis* eQTLs (±1Mb window around the transcription start site) in 48 tissues available in the GTEx v7 database that included at least 70 samples. Significant associations were selected based on a Bonferroni corrected p-value <3.0E-5 for the number of genes and tissues tested. Subsequently, the SNP rs1545300 was tested and plotted for co-localization in the three tissues with an eQTL FDR<0.2 by applying the SMR method(53) using the GWAS and GTEx eQTL summary statistics. The method includes a test whether the effect on expression observed at a SNP or at its proxies is independent of the signal observed in the GWAS, i.e. that gene expression and y are associated only because of a latent non-genetic confounding variable (SMR test), and a second test that evaluates if the eQTL and GWAS associations can be attributable to the same causative variant (HEIDI test). Significance for co-localization of the gene expression and the GWAS signals was defined by p_{SMR}<0.01, where additionally a p_{HEIDI}≥0.05 indicates the same underlying causal variant(53).

Data availability

Summary association results of the combined GWAS meta-analysis have been submitted for full download to the CHARGE dbGaP website under accession phs000930 [https://www.ncbi.nlm.nih.gov/gap].

Study approval

All subjects gave written informed consent and all participating studies were approved by the local ethics committees and followed the recommendations of the Declaration of Helsinki.

Author Contributions

Project design and analysis: W.R., T.T., A.T., M.D, E.R.B. Management of individual study: A.F.D., C.F., C.P., E.R.B., K.J.L., M.A.I., M.D., M.G., M.Z., N.P., N.V., P.B.M., P.P., P.v.d.H., S.A., S.B.F., T.D.S., T.M., T.T., W.R., Y.J. Recruitment of individual study subjects: A.F.D., G.S., H.S., I.D., M.D.,

M.Z., N.V., P.v.d.H., S.A., S.B.F. Drafting of the manuscript: A.R., A.T., B.H.S., E.R.B., M.D.B., M.E.v.d.B., T.T., W.R. Statistical methods and analysis of individual study: A.T., C.C., C.F., H.R.W., H.S., I.M.N., K.S., M.E.v.d.B., S.P. Genotyping of individual study: A.G.U., C.F., M.N., P.B.M., U.V. Interpretation of the results: A.R., A.T., B.K., C.H., E.R.B., M.D., M.D.B., T.K., T.T., W.R. Critical review of the manuscript: all authors. The authorship order among co–first authors was set alphabetically.

Acknowledgments

Detailed acknowledgments and funding sources are provided in the Supplementary Information.

The authors have declared that no conflict of interest exists.

References

1. Reinhard W et al. The early repolarization pattern: Echocardiographic characteristics in elite athletes. *Ann. Noninvasive Electrocardiol.* 2018;e12617.
2. Sinner MF et al. Association of early repolarization pattern on ECG with risk of cardiac and all-cause mortality: a population-based prospective cohort study (MONICA/KORA). *PLoS Med.* 2010;7(7):e1000314.
3. Noseworthy PA et al. The early repolarization pattern in the general population: clinical correlates and heritability. *J. Am. Coll. Cardiol.* 2011;57(22):2284–9.
4. Uberoi A et al. Early repolarization in an ambulatory clinical population. *Circulation* 2011;124(20):2208–14.
5. Trenkwalder T et al. Left ventricular geometry and function in early repolarization: results from the population-based Gutenberg Health Study. *Clin. Res. Cardiol.* [published online ahead of print: February 28, 2019]; doi:10.1007/s00392-019-01445-7
6. Haïssaguerre M et al. Sudden cardiac arrest associated with early repolarization. *N. Engl. J. Med.* 2008;358(19):2016–23.
7. Priori SG et al. HRS/EHRA/APHRS expert consensus statement on the diagnosis and management of patients with inherited primary arrhythmia syndromes: document endorsed by HRS, EHRA, and APHRS in May 2013 and by ACCF, AHA, PACES, and AEPC in June 2013. *Hear. Rhythm* 2013;10(12):1932–63.
8. Rosso R et al. J-point elevation in survivors of primary ventricular fibrillation and matched control subjects: incidence and clinical significance. *J. Am. Coll. Cardiol.* 2008;52(15):1231–8.
9. Tikkanen JT et al. Long-term outcome associated with early repolarization on electrocardiography. *N. Engl. J. Med.* 2009;361(26):2529–37.
10. Koncz I et al. Mechanisms underlying the development of the electrocardiographic and arrhythmic manifestations of early repolarization syndrome. *J. Mol. Cell. Cardiol.* 2014;68:20–8.
11. Yan GX, Antzelevitch C. Cellular basis for the electrocardiographic J wave. *Circulation* 1996;93(2):372–9.
12. Haïssaguerre M et al. Ventricular fibrillation with prominent early repolarization associated with a rare variant of KCNJ8/KATP channel. *J. Cardiovasc. Electrophysiol.* 2009;20(1):93–8.
13. Chauveau S et al. Early repolarization syndrome caused by de novo duplication of KCND3 detected by next-generation sequencing. *Hear. case reports* 2017;3(12):574–578.
14. Yao H et al. SCN1Bβ mutations that affect their association with Kv4.3 underlie early repolarization syndrome. *J. Cell. Mol. Med.* 2018;22(11):5639–5647.
15. Liu X et al. A mutation in the CACNA1C gene leads to early repolarization syndrome with incomplete penetrance: A Chinese family study. *PLoS One* 2017;12(5):e0177532.
16. Antzelevitch C et al. J-Wave syndromes expert consensus conference report: Emerging concepts and gaps in knowledge.
17. Casado Arroyo R et al. Electrophysiological Basis for Early Repolarization Syndrome. *Front.*

480 *Cardiovasc. Med.* 2018;5:161.
481 18. Nunn LM et al. Prevalence of J-point elevation in sudden arrhythmic death syndrome families. *J.*
482 *Am. Coll. Cardiol.* 2011;58(3):286–90.
483 19. Mellor G et al. The Prevalence and Significance of the Early Repolarization Pattern in Sudden
484 Arrhythmic Death Syndrome Families. *Circ. Arrhythm. Electrophysiol.* 2016;9(6).
485 doi:10.1161/CIRCEP.116.003960
486 20. Reinhard W et al. Heritability of early repolarization: a population-based study. *Circ. Cardiovasc.*
487 *Genet.* 2011;4(2):134–8.
488 21. Bastiaenen R et al. The narrow-sense and common single nucleotide polymorphism heritability of
489 early repolarization. *Int. J. Cardiol.* [published online ahead of print: October 4, 2018];
490 doi:10.1016/j.ijcard.2018.09.119
491 22. Sinner MF et al. A meta-analysis of genome-wide association studies of the electrocardiographic
492 early repolarization pattern. *Hear. Rhythm* 2012;9(10):1627–34.
493 23. Macfarlane PW et al. The Early Repolarization Pattern: A Consensus Paper. *J. Am. Coll. Cardiol.*
494 2015;66(4):470–7.
495 24. GTEx Consortium et al. Genetic effects on gene expression across human tissues. *Nature*
496 2017;550(7675):204–213.
497 25. MacArthur J et al. The new NHGRI-EBI Catalog of published genome-wide association studies
498 (GWAS Catalog) *Nucleic Acids Res.* 2017;45(D1):D896–D901.
499 26. Christophersen IE et al. Fifteen Genetic Loci Associated With the Electrocardiographic P Wave.
500 *Circ. Cardiovasc. Genet.* 2017;10(4). doi:10.1161/CIRCGENETICS.116.001667
501 27. Roselli C et al. Multi-ethnic genome-wide association study for atrial fibrillation. *Nat. Genet.*
502 2018;50(9):1225–1233.
503 28. Nielsen JB et al. Biobank-driven genomic discovery yields new insight into atrial fibrillation biology.
504 *Nat. Genet.* 2018;50(9):1234–1239.
505 29. Verweij N et al. Genetic Determinants of P Wave Duration and PR Segment *Circ. Cardiovasc.*
506 *Genet.* 2014;7(4):475–481.
507 30. Verweij N et al. Twenty-eight genetic loci associated with ST-T-wave amplitudes of the
508 electrocardiogram. *Hum. Mol. Genet.* 2016;25(10):2093–2103.
509 31. Canela-Xandri O, Rawlik K, Tenesa A. An atlas of genetic associations in UK Biobank *Nat. Genet.*
510 2018;50(11):1593–1599.
511 32. Mercer BN et al. Early Repolarization Syndrome; Mechanistic Theories and Clinical Correlates.
512 *Front. Physiol.* 2016;7:266.
513 33. Haïssaguerre M et al. Characteristics of recurrent ventricular fibrillation associated with
514 inferolateral early repolarization role of drug therapy. *J. Am. Coll. Cardiol.* 2009;53(7):612–9.
515 34. Mavragani-Tsipidou P, Scouras ZG, Haralampidis K, Lavrentiadou S, Kastritsis CD. The polytene
516 chromosomes of Drosophila triauraria and D. quadraria, sibling species of D. auraria. *Genome*
517 1992;35(2):318–26.
518 35. Haïssaguerre M et al. Depolarization versus repolarization abnormality underlying inferolateral J-
519 wave syndromes: New concepts in sudden cardiac death with apparently normal hearts. *Hear.*
520 *Rhythm* [published online ahead of print: November 2, 2018]; doi:10.1016/j.hrthm.2018.10.040
521 36. Bonasio R, Shiekhattar R. Regulation of transcription by long noncoding RNAs. *Annu. Rev. Genet.*
522 2014;48(1):433–55.
523 37. Ulitsky I. Evolution to the rescue: using comparative genomics to understand long non-coding
524 RNAs. *Nat. Rev. Genet.* 2016;17(10):601–14.
525 38. Sallam T, Sandhu J, Tontonoz P. Long Noncoding RNA Discovery in Cardiovascular Disease:
526 Decoding Form to Function. *Circ. Res.* 2018;122(1):155–166.
527 39. Harismendy O et al. 9p21 DNA variants associated with coronary artery disease impair interferon-
528 γ signalling response. *Nature* 2011;470(7333):264–8.
529 40. Broadbent HM et al. Susceptibility to coronary artery disease and diabetes is encoded by distinct,
530 tightly linked SNPs in the ANRIL locus on chromosome 9p. *Hum. Mol. Genet.* 2008;17(6):806–14.
531 41. Medeiros-Domingo A et al. Gain-of-function mutation S422L in the KCNJ8-encoded cardiac
532 K(ATP) channel Kir6.1 as a pathogenic substrate for J-wave syndromes. *Hear. Rhythm*
533 2010;7(10):1466–71.
534 42. Barajas-Martínez H et al. Molecular genetic and functional association of Brugada and early
535 repolarization syndromes with S422L missense mutation in KCNJ8 *Hear. Rhythm* 2012;9(4):548–555.
536 43. Landrum MJ et al. ClinVar: public archive of interpretations of clinically relevant variants. *Nucleic*
537 *Acids Res.* 2016;44(D1):D862-8.
538 44. Tikkanen JT et al. Early repolarization: electrocardiographic phenotypes associated with favorable
539 long-term outcome. *Circulation* 2011;123(23):2666–73.
540 45. Cheng Y-J et al. Role of Early Repolarization Pattern in Increasing Risk of Death. *J. Am. Heart*

Assoc. 2016;5(9). doi:10.1161/JAHA.116.003375
46. R Development Core Team, R Core Team. R: A Language and Environment for Statistical Computing [Internet]2016;https://www.r-project.org. cited April 2, 2016
47. Fuchsberger C, Taliun D, Pramstaller PP, Pattaro C, CKDGen consortium. GWAtoolbox: an R package for fast quality control and handling of genome-wide association studies meta-analysis data. *Bioinformatics* 2012;28(3):444–445.
48. Willer CJ, Li Y, Abecasis GR. METAL: fast and efficient meta-analysis of genomewide association scans. *Bioinformatics* 2010;26(17):2190–1.
49. Bulik-Sullivan BK et al. LD Score regression distinguishes confounding from polygenicity in genome-wide association studies. *Nat. Genet.* 2015;47(3):291–5.
50. Pe'er I, Yelensky R, Altshuler D, Daly MJ. Estimation of the multiple testing burden for genomewide association studies of nearly all common variants. *Genet Epidemiol* 2008;32(4):381–385.
51. Higgins JPT, Thompson SG, Deeks JJ, Altman DG. Measuring inconsistency in meta-analyses. *BMJ* 2003;327(7414):557–560.
52. Yang J, Lee SH, Goddard ME, Visscher PM. GCTA: a tool for genome-wide complex trait analysis. *Am. J. Hum. Genet.* 2011;88(1):76–82.
53. Zhu Z et al. Integration of summary data from GWAS and eQTL studies predicts complex trait gene targets. *Nat. Genet.* 2016;48(5):481–7.
54. Pruim RJ et al. LocusZoom: regional visualization of genome-wide association scan results. *Bioinformatics* 2010;26(18):2336–7.
55. Dreszer TR et al. The UCSC Genome Browser database: extensions and updates 2011. *Nucleic Acids Res* 2012;40(Database issue):D918--D923.

Figure Legends

Figure 1. GWAS results of the *KCND3* locus

The results of the combined early repolarization pattern (ERP) GWAS results for the *KCND3* locus are shown for the replicated discovery stage lead SNP rs12090194 in n=38,811 individuals (A and B), and for the combined GWAS lead SNP rs1545300 in n=38,806 individuals (C and D). The regional association plots (A and C) show the association results in a ±500 kb region around the lead SNP. SNPs are plotted on the x-axis according to their chromosomal position with the $-\log_{10}$(p-value) of the GWAS association on the y-axis. Correlation with the lead SNP (purple) is estimated based on the 1000 Genomes reference samples. Plots were generated using the website of LocusZoom(54). Genetic positions refer to GRCh37/hg19 coordinates. Forest plots of the respective lead SNPs are provided in (B) and (D), with odds ratios and their 95% confidence intervals plotted on the x-axis. I^2 is the percentage of total variation across studies that is due to heterogeneity.

Figure 2. Location of the significantly associated SNPs within the *KCND3* gene

The top 43 SNPs with a genome-wide significance visualized by UCSC Genome Browser(55). All SNPs mapped into *KCND3* gene. The two leads SNPs rs1545300 and rs12090194 of the discovery and combined meta-analyses are reported with a red and an orange diamond, respectively. The H3K27Ac mark track (Layered H3K27Ac) shows the levels of enrichment of the H3K27Ac histone mark. Chemical modifications (e.g. methylation and acylation) to the histone proteins present in chromatin influence gene expression by changing how accessible the chromatin is to transcription. The H3K27Ac histone mark is thought to enhance transcription possibly by blocking the spread of the repressive histone mark H3K27Me3. The GeneHancer (GH) track set shows human regulatory elements, i.e. enhancers (gray) and promoters (red), containing tracks representing regulatory elements (Reg Elems), gene transcription start sites (TSS), associations between regulatory elements and genes (Interactions), and clustered interactions (Clusters). A gray box in the DNaseI Hypersensitivity Clusters track (DNase Clusters) indicates the extent of the hypersensitive region with darkness proportional to the maximum signal strength observed in any cell line. A gray box in the Transcription Factor ChIP-seq Clusters track (Txn Factor ChIP) indicates a cluster of transcription factor occupancy, with the darkness of the box being proportional to the maximum signal strength observed in any cell line contributing to the cluster.

Figure 3. Co-localization results

Illustration of the SMR test for the early repolarization pattern (ERP) risk and the expression quantitative trait loci (eQTLs) at the rs1545300 locus at chromosome 1p13.2 for (A) left ventricle of the heart, (B) tibial artery, and (C) minor salivary gland tissue. The sample size for the eQTLs are n=272, n=388 and n=85 in panels (A), (B) and (C), respectively. In each panel, the upper box shows the GWAS regional association plot with ERP risk of the combined GWAS (n=39,456), with level of significance of the SMR test (y-axis) for each transcript in the locus indicated by a diamond positioned at the center of the transcript. A significant SMR test represented by a purple diamond indicates an association of the transcript level of the respective genes (purple label) with the trait. For all three tissues, an increased gene expression level of a significant SMR test was associated with a higher risk of ERP. A filled purple diamond indicates a HEIDI test p-value >0.05, thus a likely co-localization. The lower box shows the regional association distribution with changes in expression of the highlighted (purple) gene transcript in the respective tissue. In both boxes, the x-axis refers to GRCh37/hg19 genomic coordinates.

608 **Table 1: Baseline characteristics of the study populations**

Study	Subgroup	Number of samples (n)	Number of females (n)	Age in years (mean±SD)	Heart rate in bpm (mean±SD)	BMI (mean±SD)
Discovery stage						
BRIGHT	ERP+	189	105	57.6±12.1	61.7±9.9	27.7±3.4
	ERP-	1173	747	59.4±12.3	63.7±11.2	27.4±3.8
GHS1	ERP+	182	60	54.5±10.0	67.6±11.5	26.8±4.4
	ERP-	2628	1358	55.6±10.9	69.1±10.8	27.1±4.7
GHS2	ERP+	70	26	54.0±10.2	67.1±11.4	27.5±5.5
	ERP-	1028	536	54.9±10.9	68.7±10.8	27.2±4.9
GRAPHIC	ERP+	57	18	52.3±3.9	63.5±8.0	27.4±4.0
	ERP-	893	457	52.8±4.5	64.1±9.8	27.4±4.3
Lifelines	ERP+	1253	639	48.0±11.5	66.3±10.9	25.7±3.8
	ERP-	11463	6902	47.9±11.3	68.4±11.5	26.4±4.3
SHIP	ERP+	173	79	46.6±16.1	70.5±11.6	25.9±4.2
	ERP-	2835	1508	48.5±15.8	73.7±11.6	27.3±4.9
SHIP-Trend	ERP+	86	38	49.8±14.5	64.4±8.9	26.9±4.4
	ERP-	848	494	49.7±13.4	65.9±9.6	27.3±4.6
TwinsUK	ERP+	171	150	51.7±13.2	64.1±10.3	25.3±4.4
	ERP-	2773	2651	52.7±12.4	66.8±10.4	25.7±4.6
Replication stage						
CHRIS	ERP+	427	159	45.2±16.3	60.3±8.9	25.4±4.2
	ERP-	3953	2318	45.7±16.1	62.5±8.8	25.6±4.6
Rotterdam Study I	ERP+	308	182	66.4±7.6	68.7±11.6	27.5±7.4
	ERP-	4438	2739	66.3±7.7	69.2±11.9	27.1±6.9
Rotterdam Study II	ERP+	164	84	64.1±7.3	67.5±10.6	27.5±4.1
	ERP-	1476	825	64.4±7.5	68.8±10.8	27.5±4.1
Rotterdam Study III	ERP+	225	116	56.7±5.6	69.0±11.7	27.6±4.9
	ERP-	2643	1541	57.0±6.7	69.6±10.5	27.5±5.0

609

610 ERP+: cases with early repolarization pattern; ERP-: controls

611 **Table 2: Lead SNPs of the GWAS association results**

					Discovery				Replication				Combined			
SNP	Chr:position	A1/ A2	Nearest gene	AF1	OR	P	I^2	N	OR	P	I^2	N	OR	P	I^2	N
rs12090194	1:112,454,822	t/c	*KCND3*	0.32	0.80 [0.75-0.86]	**4.6E-10**	34	25177	0.86 [0.79-0.95]	2.5E-03	39	13634	0.82 [0.78-0.87]	9.3E-12	35	38811
rs1545300	1:112,464,004	t/c	*KCND3*	0.32	0.81 [0.75-0.86]	1.4E-09	41	25172	0.85 [0.77-0.94]	9.4E-04	56	13634	0.82 [0.78-0.87]	**7.7E-12**	43	38806
rs139772527	16:208,761	t/c	*HBZ*	0.01	2.57 [1.85-3.58]	**2.0E-08**	0	21495	1.21 [0.85-1.73]	2.8E-01	0	13634	1.81 [1.42-2.31]	1.4E-06	11	35129

612

613 A1: effect allele; AF1: allele frequency of A1; Chr: chromosome; position: position corresponding to
614 build 37 (GRCh37); OR: odds ratio of A1 [95% confidence interval]; P: association p-value; I^2:
615 percentage of total variation across studies that is due to heterogeneity; N: sample size. Bold values
616 indicate the lead SNP (lowest p-value) of a significantly associated locus in the corresponding meta-
617 analysis stage.
618

Table 3: The 43 genome-wide significant SNPs of the *KCND3* locus

SNP	position	location	A1/A2	AF1	OR	P
rs817972	112,399,057	intron	a/g	0.90	1.35 [1.22-1.50]	2.0E-08
rs583731	112,421,854	intron	t/c	0.09	0.69 [0.62-0.77]	3.6E-11
rs528779	112,424,077	intron	t/c	0.71	1.18 [1.11-1.25]	2.0E-08
rs612790	112,426,577	intron	c/g	0.29	0.84 [0.80-0.89]	1.1E-08
rs2813862	112,427,918	intron	c/g	0.29	0.84 [0.79-0.89]	5.9E-09
rs1767283	112,428,953	intron	t/c	0.29	0.84 [0.80-0.89]	8.5E-09
rs11102354	112,433,666	intron	a/g	0.31	1.18 [1.11-1.25]	3.3E-08
rs605604	112,433,863	intron	a/c	0.70	1.19 [1.12-1.26]	6.4E-09
rs2798334	112,437,344	intron	t/c	0.30	0.84 [0.79-0.89]	7.7E-09
rs2813864	112,437,853	intron	a/g	0.29	0.84 [0.79-0.89]	8.2E-09
rs2587368	112,437,907	intron	t/c	0.40	0.86 [0.81-0.90]	1.7E-08
rs2813865	112,437,956	intron	a/g	0.25	0.82 [0.77-0.87]	8.6E-10
rs894849	112,437,964	intron	t/c	0.41	0.86 [0.81-0.90]	1.3E-08
rs608673	112,439,757	intron	t/c	0.44	0.86 [0.81-0.91]	2.0E-08
rs7539683	112,439,770	intron	t/g	0.27	1.20 [1.13-1.27]	2.0E-09
rs1805222	112,440,983	intron	a/g	0.27	1.20 [1.13-1.27]	3.3E-09
rs2120436	112,451,447	intron	t/c	0.32	0.82 [0.78-0.87]	1.7E-11
rs2034124	112,451,681	intron	a/g	0.45	1.16 [1.10-1.22]	1.6E-08
rs12090194	112,454,822	intron	t/c	0.32	0.82 [0.78-0.87]	9.3E-12
rs72692596	112,455,415	intron	t/c	0.32	0.84 [0.79-0.89]	2.8E-09
rs72692597	112,455,442	intron	t/g	0.32	0.84 [0.79-0.89]	2.9E-09
rs4839182	112,456,538	intron	a/g	0.55	1.18 [1.12-1.25]	3.9E-09
rs4839183	112,456,882	intron	a/g	0.46	1.17 [1.11-1.23]	5.3E-09
rs72692602	112,458,833	intron	t/c	0.68	1.20 [1.13-1.27]	2.5E-09
rs72694603	112,458,893	intron	t/c	0.32	0.83 [0.79-0.89]	2.3E-09
rs4839184	112,460,221	intron	c/g	0.32	0.83 [0.78-0.87]	2.6E-11
rs4839185	112,460,262	intron	t/c	0.68	1.21 [1.15-1.28]	1.4E-11
rs1443926	112,461,902	intron	a/g	0.68	1.21 [1.15-1.28]	2.0E-11
rs6682872	112,462,984	intron	a/g	0.60	1.18 [1.12-1.24]	9.6E-10
rs4838926	112,463,323	intron	c/g	0.40	0.85 [0.81-0.90]	2.0E-09
rs4838927	112,463,617	intron	t/c	0.60	1.18 [1.12-1.24]	1.7E-09
rs1545300	112,464,004	intron	t/c	0.32	0.82 [0.78-0.87]	7.7E-12
rs17029069	112,464,376	intron	t/c	0.30	1.21 [1.14-1.28]	1.1E-10
rs12119724	112,468,814	intron	t/c	0.29	1.21 [1.14-1.28]	7.3E-11
rs11588747	112,470,474	intron	t/c	0.70	1.19 [1.12-1.27]	1.5E-08
rs2010749	112,470,581	intron	t/c	0.63	1.20 [1.14-1.27]	3.7E-11
rs1443927	112,471,029	intron	c/g	0.69	1.20 [1.14-1.28]	1.9E-10
rs12145374	112,480,536	intron	a/c	0.80	1.22 [1.14-1.30]	8.6E-09
rs72694622	112,481,667	intron	t/c	0.18	0.81 [0.75-0.87]	3.6E-08
rs12144965	112,484,962	intron	t/c	0.82	1.23 [1.14-1.32]	2.8E-08
rs3008527	112,523,095	intron	t/c	0.70	1.19 [1.12-1.26]	5.8E-09
rs3008528	112,527,869	intron	a/t	0.70	1.18 [1.11-1.25]	1.7E-08
rs2075811	112,530,626	intron	c/g	0.30	0.85 [0.80-0.90]	1.7E-08

621 A1: effect allele; AF1: allele frequency of A1; position on chromosome 1 (build 37, GRCh37); OR:
622 odds ratio of A1 [95% confidence interval]; P: association p-value. The SNPs are ordered by their
623 position, and the results of the combined meta-analysis are given.

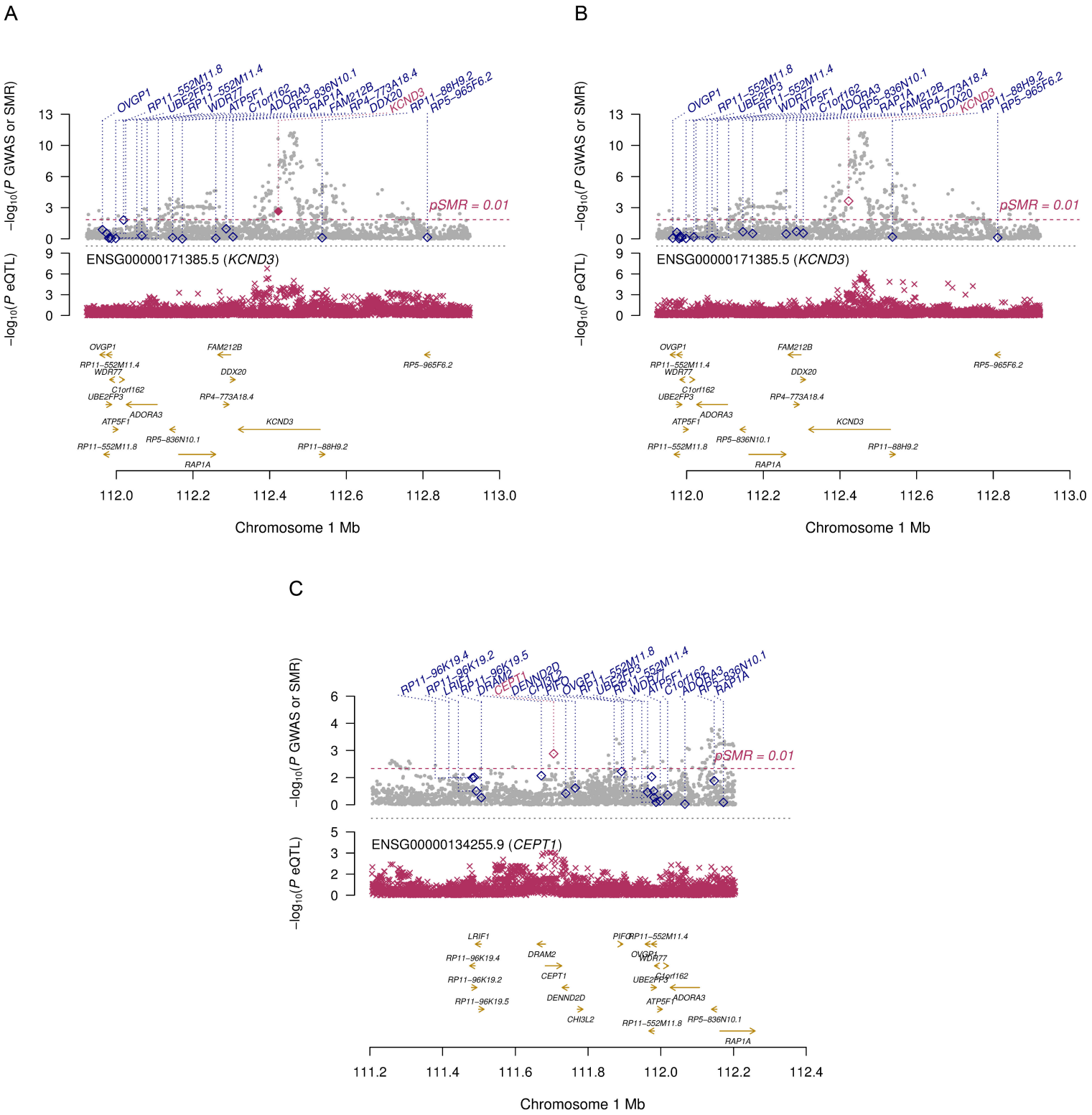
A
B
C
−log10(P GWAS or SMR)
−log10(P eQTL)
pSMR = 0.01
ENSG00000171385.5 (KCND3)
ENSG00000134255.9 (CEPT1)
OVGP1
RP11−552M11.8
UBE2FP3
RP11−552M11.4
WDR77
ATP5F1
C1orf162
ADORA3
RP5−836N10.1
RAP1A
FAM212B
RP4−773A18.4
DDX20
KCND3
RP11−88H9.2
RP5−965F6.2
RP11−96K19.4
RP11−96K19.2
LRIF1
RP11−96K19.5
DRAM2
CEPT1
DENND2D
CHI3L2
PIFO
Chromosome 1 Mb

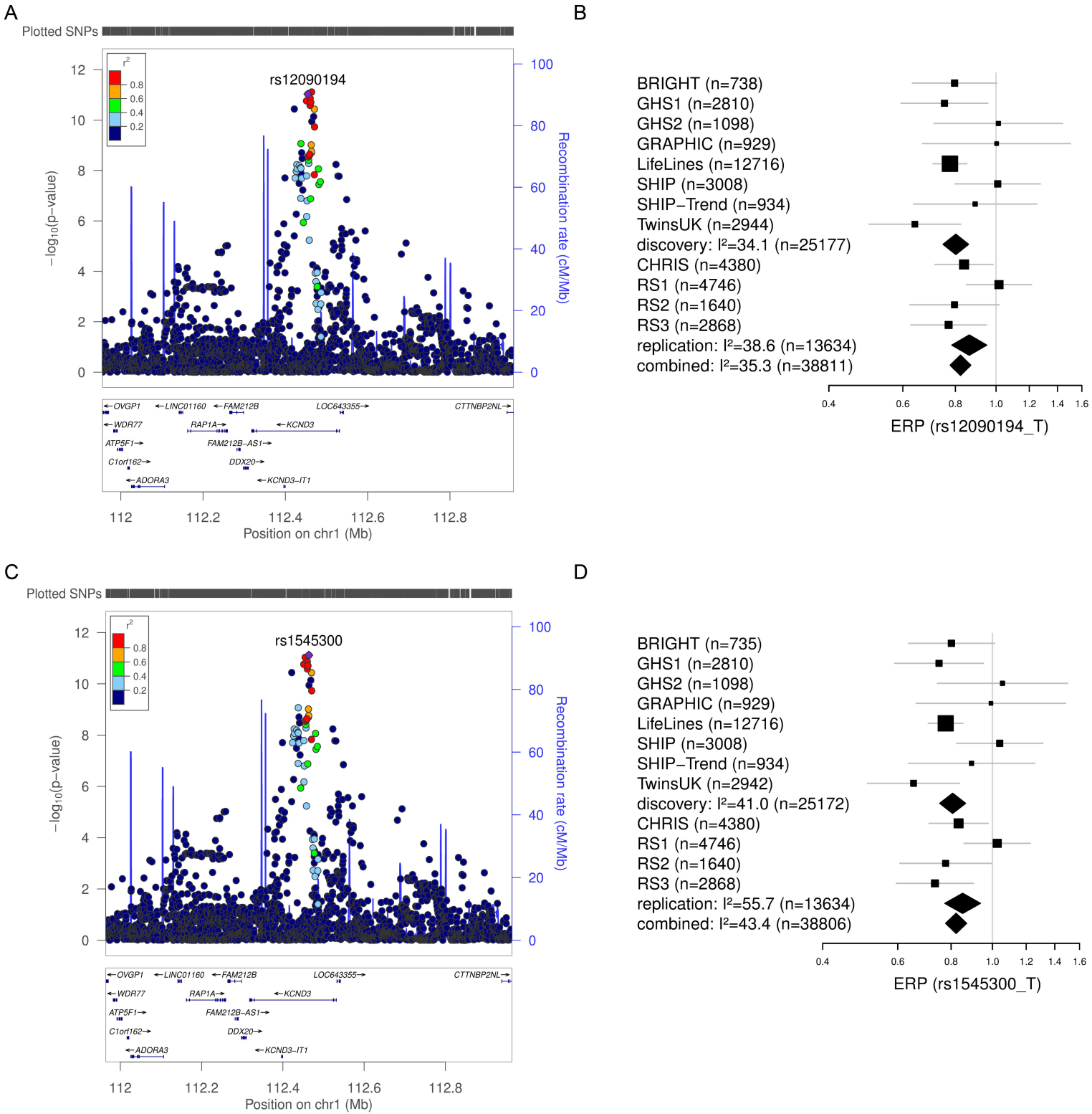
A
Plotted SNPs
rs12090194
r²
0.8
0.6
0.4
0.2
−log10(p−value)
Recombination rate (cM/Mb)
OVGP1
LINC01160
FAM212B
LOC643355
CTTNBP2NL
WDR77
RAP1A
KCND3
ATP5F1
FAM212B−AS1
C1orf162
DDX20
ADORA3
KCND3−IT1
Position on chr1 (Mb)
B
BRIGHT (n=738)
GHS1 (n=2810)
GHS2 (n=1098)
GRAPHIC (n=929)
LifeLines (n=12716)
SHIP (n=3008)
SHIP−Trend (n=934)
TwinsUK (n=2944)
discovery: I²=34.1 (n=25177)
CHRIS (n=4380)
RS1 (n=4746)
RS2 (n=1640)
RS3 (n=2868)
replication: I²=38.6 (n=13634)
combined: I²=35.3 (n=38811)
ERP (rs12090194_T)
C
Plotted SNPs
rs1545300
Position on chr1 (Mb)
D
BRIGHT (n=735)
GHS1 (n=2810)
GHS2 (n=1098)
GRAPHIC (n=929)
LifeLines (n=12716)
SHIP (n=3008)
SHIP−Trend (n=934)
TwinsUK (n=2942)
discovery: I²=41.0 (n=25172)
CHRIS (n=4380)
RS1 (n=4746)
RS2 (n=1640)
RS3 (n=2868)
replication: I²=55.7 (n=13634)
combined: I²=43.4 (n=38806)
ERP (rs1545300_T)

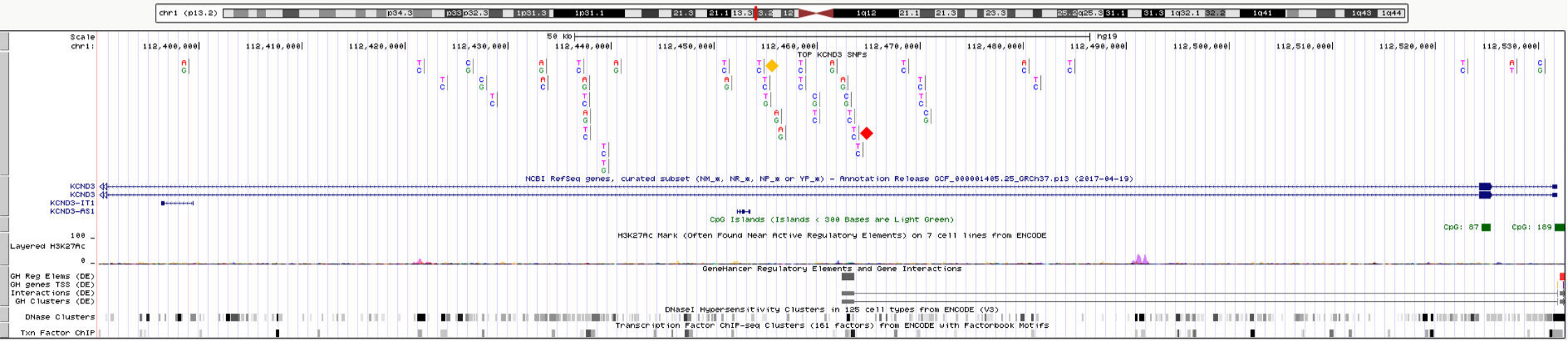
chr1 (p13.2)
Scale
chr1:
50 kb
hg19
112,400,000
112,410,000
112,420,000
112,430,000
112,440,000
112,450,000
112,460,000
112,470,000
112,480,000
112,490,000
112,500,000
112,510,000
112,520,000
112,530,000
TOP KCND3 SNPs
NCBI RefSeq genes, curated subset (NM_*, NR_*, NP_* or YP_*) - Annotation Release GCF_000001405.25_GRCh37.p13 (2017-04-19)
KCND3
KCND3
KCND3-IT1
KCND3-AS1
CpG Islands (Islands < 300 Bases are Light Green)
CpG: 87
CpG: 109
100
H3K27Ac Mark (Often Found Near Active Regulatory Elements) on 7 cell lines from ENCODE
Layered H3K27Ac
0
GeneHancer Regulatory Elements and Gene Interactions
GH Reg Elems (DE)
GH genes TSS (DE)
Interactions (DE)
GH Clusters (DE)
DNaseI Hypersensitivity Clusters in 125 cell types from ENCODE (V3)
DNase Clusters
Transcription Factor ChIP-seq Clusters (161 factors) from ENCODE with Factorbook Motifs
Txn Factor ChIP